

## An inherent structure view of liquid-vapor interfaces

Frank H. Stillinger<sup>a)</sup>

*Department of Chemistry, Princeton University, Princeton, New Jersey 08544, USA*

(Received 8 February 2008; accepted 27 March 2008; published online 27 May 2008)

The formal statistical mechanical theory describing liquid-vapor interfaces at thermal equilibrium has been incomplete, owing partly to discrepancies between two primary views, the local free energy approach originated by van der Waals and the capillary wave approach initiated by Mandelstam. The former provides detailed prescriptions for interfacial density profiles and surface tensions, and has recently been tailored to conform to nonclassical critical phenomena. The latter postulates a crude discontinuous density profile that is geometrically delocalized by surface excitations, but which qualitatively incorporates basic gravitational effects that are missing in the van der Waals method. The present analysis provides a formalism within which both approaches can be reconciled. It draws upon the inherent structure mapping procedure to define an intrinsic liquid-vapor density profile which invokes no arbitrary parameters that are not already present in the many-particle potential energy function or its thermodynamics. By construction, this intrinsic profile plays a role conventionally given to a van der Waals interface profile, and although it is free of capillary waves it can serve as a starting point for evaluating the gravitational implications of those interfacial fluctuation effects. © 2008 American Institute of Physics. [DOI: 10.1063/1.2911926]

### I. INTRODUCTION

Interfaces between coexisting stable phases present a wide range of phenomena and require a correspondingly wide array of theoretical methods for their analyses. The present paper focuses just on planar liquid-vapor interfaces for single-component systems. In spite of a long and well-embellished history for this case,<sup>1-3</sup> its basic statistical mechanical theory is not yet a closed subject. The objective of the present paper is to bridge a conceptual gap between two distinct approaches to understanding the matter density distribution across the interface. The general “inherent structure” representation for many-body systems<sup>4-7</sup> supplies the context for this analysis.

The following section (Sec. II) provides rudimentary outlines for the two main theoretical approaches to prediction of liquid-vapor interfacial density profiles, to highlight strategic differences between them. Specifically, Sec. II A outlines the key elements of the venerable van der Waals interface theory<sup>8</sup> which has benefited from more recent statistical mechanical refinements.<sup>3</sup> Section II B offers an analogous brief overview for the “capillary wave” theory of interface diffuseness.<sup>9,10</sup>

Section III indicates the way in which the inherent structure formalism naturally adapts to liquid-vapor coexistence and to the interface it involves. In particular, this formalism explicitly incorporates the gravitational field acting on the phase-separated many-body system. Section III also describes how the Gibbs equimolar dividing surface<sup>11</sup> behaves under the configurational steepest descent mapping that plays a central role in the inherent structure representation. For simplicity, this formalism is developed for the case of structureless particles.

The technique for separation of inherent structures (and their associated basins of attraction) into those that do, and those that do not, contain capillary wave deformations appears in Sec. IV. This leads to the natural definition of an intrinsic density profile that appears to be well suited to play the role originally intended for the van der Waals density profile. All other inherent structures not contributing to this intrinsic profile conceivably might be classified by their capillary wave amplitudes, but this classification is not entirely straightforward as explained in Sec. V. It is significant that the proposed method for identification of an intrinsic profile is completely free of any arbitrary or unnatural introduced parameters (length scales, energies, etc.) that are not directly or indirectly generated by the system’s own potential energy function. In this respect, the present approach distinguishes itself from some other analyses that have been directed toward reconciling the two prior theoretical approaches and to defining an intrinsic profile.<sup>12-15</sup>

Concluding remarks of several kinds appear in the final section (Sec. VI). These include comments about application of the present strategy to other classes of interfaces, such as those for molecular liquids, for liquid solutions, and for pairs of immiscible liquids. Section VI also presents suggestions for future experimental and simulational investigations related to the approach advocated in this paper.

The formal context used in the following analysis is that of classical statistical mechanics. This is not a fundamental restriction, however. An extension to include quantum effects is feasible, and would certainly be required for a proper description of the cases presented by the liquid-vapor interfaces of the helium isotopes.<sup>16</sup>

### II. BACKGROUND

In order to provide a suitable setting for the inherent structure approach to be introduced below, this presentation

<sup>a)</sup>Electronic mail: fhs@princeton.edu.

begins with brief summaries of two distinct predictive viewpoints that appear to be somewhat at odds with one another. Both of these viewpoints individually offer important insights, but each falls short of a complete and accurate description of the interface problem. Consequently, they need to be placed in a more comprehensive context of general statistical mechanical theory. In summarizing each of these approaches, coordinate  $z$  will measure vertical position in the system, and the density profile through both bulk phases and the planar interface separating them will be denoted by  $\rho(z)$ .

### A. Van der Waals approach

The basic assumption underlying the van der Waals view is that  $\rho(z)$  represents a free-energy-minimizing compromise between two competing effects. One of these is the free energy increase that is associated with any local particle density that lies between the coexistence densities  $\rho_v, \rho_l$  of the bulk vapor and liquid phases, respectively. The other is associated with the nonzero size of molecules and of their interaction range, which would make it costly to establish an abrupt density discontinuity at the interface. The compromise in its simplest version involves identifying that  $\rho(z)$  which minimizes the following functional combining the two competing effects:<sup>17</sup>

$$F\{\rho(z)\} = \int_{-\infty}^{+\infty} \{-W[\rho(z)] + (m_0/2)[\rho'(z)]^2\} dz, \quad (\text{II.1})$$

subject to the boundary conditions

$$\begin{aligned} \lim_{z \rightarrow +\infty} \rho(z) &= \rho_v, \\ \lim_{z \rightarrow -\infty} \rho(z) &= \rho_l. \end{aligned} \quad (\text{II.2})$$

In expression (II.1) the positive quantity  $m_0$  is determined by the range of molecular interactions, and  $-W$  stands for the increment in Helmholtz free energy per unit volume above the linear interpolation between its values at the coexistence number densities  $\rho_v$  and  $\rho_l$ .

Variational minimization of  $F\{\rho(z)\}$  in Eq. (II.1) leads to the differential equation

$$m_0 \rho''(z) + W'[\rho(z)] = 0. \quad (\text{II.3})$$

A simple yet qualitatively appealing form to choose for  $W$  is a quartic polynomial in  $\rho$  that vanishes at  $\rho_l$  and at  $\rho_v$ ,

$$W(\rho) = -w_0[(2\rho - \rho_l - \rho_v)^2 - (\rho_l - \rho_v)^2]^2, \quad (\text{II.4})$$

where  $w_0$  is a positive constant. In particular, this form is consistent with the well-known van der Waals equation of state in the neighborhood of its critical point. After inserting expression (II.4) into differential Eq. (II.3) and treating  $m_0$  as constant, it is straightforward to verify that the solutions satisfying the boundary conditions (II.2) are

$$\rho(z) = \left( \frac{\rho_l + \rho_v}{2} \right) - \left( \frac{\rho_l - \rho_v}{2} \right) \tanh[(8w_0/m_0)^{1/2}(\rho_l - \rho_v)(z - z_0)]. \quad (\text{II.5})$$

Here,  $z_0$  is the arbitrary altitude of the center of the interface.

Upon approach to the liquid-vapor critical point where the two bulk-phase densities each converge to the critical density  $\rho_c$ , Eq. (II.5) predicts that the interface will widen without bound, in agreement with experimental observations.<sup>18,19</sup> Although the specific functional form in Eq. (II.5) depends on the assumed free energy density expression [Eq. (II.4)], any qualitatively similar expression would lead to the same conclusion about critical-region widening. In particular, more appropriate forms for  $m_0$  and  $W(\rho)$  can be assigned that are consistent with nonclassical critical point phenomena,<sup>3,20</sup> but the resulting shape of the interfacial density profile continues qualitatively to resemble the monotonic function shown in Eq. (II.5).

From the standpoint of the inherent structure analysis to be developed below, it is significant that the gravitational field makes no explicit appearance in this van der Waals approach, and so is absent from the predicted interface profile. It should also be pointed out that a local imbalance of attractive dispersion forces in the interfacial zone will generate density perturbations varying asymptotically as  $|z|^{-3}$  that do not appear in Eq. (II.5), but that an extended version of functional (II.1) beyond its square-gradient format will capture this effect.

### B. Capillary wave approach

By contrast with the van der Waals formalism, the capillary wave picture places its principal emphasis on the gravitational field and its influence on the interfacial matter distribution. It is important to note that the strength  $g$  of this external field can vary very widely from its familiar terrestrial value ( $g \cong 980 \text{ cm/s}^2$ ) depending on the alternative physical circumstances. In an orbiting space station environment, it effectively vanishes. However, ultracentrifuges can provide the equivalent of up to  $10^6$  times the normal terrestrial value.<sup>21</sup> Neutron stars offer an extreme example, with  $g$  at their surfaces in the neighborhood of  $10^{11}$  times the terrestrial surface strength.<sup>22</sup>

The elementary version of capillary wave theory presumes that there exists an underlying (unexcited) flat density profile, and that this profile can be regarded naively but adequately as a simple density discontinuity at height  $z_0$  between the bulk-phase values  $\rho_l$  and  $\rho_v$ . Furthermore, this “undisturbed” profile is assumed to possess a surface tension  $\gamma_0 > 0$ . In addition, the initially planar shape can be altered by thermally excited vertical displacements. These displacements can be resolved into superpositions of sinusoidal surface waves. Provided that such surface waves have small amplitudes, they should act as independent normal modes. A typical surface wave with two-dimensional wavevector  $\mathbf{k} \equiv (k_x, k_y)$  would produce the following vertical displacement pattern:

$$\Delta z(x, y) = a(\mathbf{k}) \sin(k_x x + k_y y), \quad (\text{II.6})$$

where  $x$  and  $y$  are the horizontal position coordinates. The incremental energy  $\varepsilon(\mathbf{k})$  associated with this capillary wave normal mode involves a part associated with a surface area increase, and a part arising from work against the gravita-

tional field. Both parts are quadratic in the wave amplitude so that

$$\varepsilon(\mathbf{k}) = [\gamma_0 k^2 + mg(\rho_l - \rho_v)] [Aa^2(\mathbf{k})/4]. \quad (\text{II.7})$$

Here,  $m$  is the particle mass and  $A$  is the nominal (undisturbed) interface area.

Owing to the fact that the interface arises from the spatial arrangements of discrete atomic or molecular entities, the capillary wave approach is obliged to recognize the necessity for an upper wavevector cutoff,

$$|\mathbf{k}| \leq k_u, \quad (\text{II.8})$$

determined approximately by a molecular-scale length. With this restriction, it is straightforward to evaluate the mean-square vertical displacement of the surface due to the contributions from the independent capillary waves at temperature  $T$ . In the limit that surface area  $A$  becomes arbitrarily large in both  $x$  and  $y$  directions, the result is the following:

$$\langle (\Delta z)^2 \rangle = \frac{k_B T}{4\pi\gamma_0} \ln \left[ \frac{\gamma_0 k_u^2}{mg(\rho_l - \rho_v)} + 1 \right]. \quad (\text{II.9})$$

The corresponding effect of the capillary waves on the density profile is to broaden the assumed undisturbed density discontinuity to an error-function form,

$$\rho(z) = \left( \frac{\rho_l + \rho_v}{2} \right) - \left( \frac{\rho_l - \rho_v}{2} \right) \text{erf} \left( \frac{z}{[2\langle (\Delta z)^2 \rangle]^{1/2}} \right). \quad (\text{II.10})$$

As noted above for the simple version of the van der Waals approach, this form also fails to display the expected  $|z|^{-3}$  asymptotic deviations from the bulk-phase densities due to interparticle dispersion attractions.

The capillary wave approach makes no predictions about the temperature dependence of the density difference  $\rho_l - \rho_v$  nor of the surface tension  $\gamma_0$ , though it implicitly assumes that both continuously vanish as the critical temperature is approached from below. That being the case, then in qualitative agreement with the van der Waals approach it implies that the interface width diverges at the critical point. But unlike the van der Waals theory, it also implies that even below the critical temperature, the width diverges as the gravitational field strength  $g$  approaches zero, an attribute that is clear from Eqs. (II.9) and (II.10) above. It should be stressed that this  $g \rightarrow 0$  width divergence is produced primarily by the long-wavelength capillary waves, precisely those for which the assumption of independence as normal modes is most justifiable.

Clearly, the underlying assumption of a density discontinuity from  $\rho_l$  to  $\rho_v$  for an undisturbed interface as invoked by the capillary wave picture is crude. So too is the presumption of independence for all of the capillary wave excitation modes with wavelengths greater than an imprecisely defined cutoff specified by  $k_u$ . There is no provision for handling overhanging particle extrusions. Nevertheless, this approach does seem to capture some basic features of liquid-vapor interface physics that must appear in some form within a complete theory.

### C. Prospects for resolution

It has been suggested that the van der Waals and the capillary wave views of the interface phenomena might be combined in an elementary manner. Specifically, the observable density profile might consist of a van der Waals intrinsic profile that has been further broadened by capillary wave modes. At least some experimental light scattering studies have qualitatively supported this notion.<sup>23,24</sup> However, no convincing argument has yet been forthcoming to demonstrate that the density profile assigned by a van der Waals approach is itself completely devoid of the effects of capillary wave degrees of freedom. The following analysis has been designed to avoid that kind of conceptual ambiguity.

### III. INHERENT STRUCTURE FORMALISM

To begin we consider first a fixed number  $N$  of identical structureless particles confined to a rectangular box of volume  $V = L_x L_y L_z$ , whose horizontal cross-sectional area is  $A = L_x L_y$ . The “floor” and “ceiling” will be impenetrable walls. For analytical convenience, periodic boundary conditions will apply in the lateral ( $x, y$ ) directions. A basic statistical mechanical analysis starts with specification of the interactions operating in the system of interest. For the present case, the potential energy function adopts the form

$$\Phi_g(\mathbf{r}_1 \dots \mathbf{r}_N) = \Phi(\mathbf{r}_1 \dots \mathbf{r}_N) + mg \sum_{i=1}^N z_i. \quad (\text{III.1})$$

In this expression  $\mathbf{r}_i \equiv (x_i, y_i, z_i)$  locates particle  $i$ , the particle mass is  $m$  as earlier, and  $\Phi$  represents the total interaction potential of the particles among themselves and with the impenetrable floor and ceiling barriers. Both  $\Phi$  and  $\Phi_g$  are fully symmetric with respect to all permutations of particle positions on account of the identity of the  $N$  particles. In order for a thermodynamic liquid-vapor transition to exist,  $\Phi$  must contain sufficiently strong and long-ranged attractions between the particles. Assuming that  $g > 0$ , the denser of the two coexisting phases will lie at lower  $z$  in  $V$  than the less dense one. This spatial asymmetry can be extended to  $g = 0$  by making the “floor” locally attracting for particles, and the “ceiling” locally repelling.

Within the domain of classical statistical mechanics, the probability distribution for the system to exist in the configuration  $\mathbf{r}_1 \dots \mathbf{r}_N$  is given by the normalized Boltzmann factor,

$$P(\mathbf{r}_1 \dots \mathbf{r}_N) = \exp[-\Phi_g(\mathbf{r}_1 \dots \mathbf{r}_N)/k_B T] / Z. \quad (\text{III.2})$$

The normalization factor  $Z$  is the classical canonical partition function for configurational coordinates,

$$Z = \int_V d\mathbf{r}_1 \dots \int_V d\mathbf{r}_N \exp[-\Phi_g(\mathbf{r}_1 \dots \mathbf{r}_N)/k_B T]. \quad (\text{III.3})$$

The vertical density profile within the system volume  $V$  can formally be obtained by integrating this probability distribution as follows:

$$\rho(z) = N \int_V d\mathbf{r}_1 \dots \int_V d\mathbf{r}_N \delta(z - z_1) P(\mathbf{r}_1 \dots \mathbf{r}_N). \quad (\text{III.4})$$

Similarly, pair, triplet, ..., particle distribution functions can formally be obtained as appropriate integrals of the full probability distribution function.

It is often useful to split the multidimensional configuration space for  $N$ -body systems exhaustively into a discrete set of basins surrounding relative minima (“inherent structures”) of the potential energy function.<sup>7,25–27</sup> This is effected by a steepest descent mapping that connects configurations of the particles to a nearby inherent structure by a continuous path on the potential energy hypersurface. In the present circumstance, the mapping is generated by the following set of coupled differential equations ( $1 \leq i \leq N$ ):

$$d\mathbf{r}_i/ds = -\nabla_i \Phi_g(\mathbf{r}_1 \dots \mathbf{r}_N), \quad (\text{III.5})$$

where  $s \geq 0$  amounts to a virtual “time” during the descent, and (except for a zero-measure set of initial conditions) the  $s \rightarrow +\infty$  limit causes the trajectory to converge onto an inherent structure. The basin of attraction for any inherent structure is defined as the set of configurations serving as initial conditions that map onto that inherent structure via Eq. (III.5). Basin geometry is substantially influenced by the presence of interparticle attractions that obviously must be present to produce liquid-vapor coexistence. Steepest descent mapping removes intrabasin vibrational displacement, and typically enhances the configurational order present in the  $N$ -particle system. It should be mentioned that the horizontal-direction periodicity selected for the present application implies that the inherent structures are not isolated points in the  $3N$ -dimensional configuration space for the  $N$  particles, but are two-dimensional manifolds resulting from the system’s horizontal translation freedom. Furthermore, permutation symmetry causes virtually all inherent structures to belong to a family of  $N!$  equivalent structures.

Suppose every member of the canonical ensemble whose configurational probability is  $P(\mathbf{r}_1 \dots \mathbf{r}_N)$  has been subjected to the steepest descent mapping. The resulting mapped ensemble consists only of the discrete set of inherent structures, and their weights are just those of the basin occupancies in the premapped ensemble. The resulting configurational probability will be denoted by  $P^{(0)}(\mathbf{r}_1 \dots \mathbf{r}_N)$ . This leads to the density profile for inherent structures by the direct analog of Eq. (III.4),

$$\rho^{(0)}(z) = N \int_V d\mathbf{r}_1 \dots \int_V d\mathbf{r}_N \delta(z - z_1) P^{(0)}(\mathbf{r}_1 \dots \mathbf{r}_N). \quad (\text{III.6})$$

One aspect of intrabasin vibrational displacement is thermal excitation acting to resist the gravitational field. This obviously affects the overall matter distribution within volume  $V$ . In particular, the centroid (center of gravity) for profile  $\rho(z)$  will generally occur at a different altitude than that for  $\rho^{(0)}(z)$ , and for conventional fluids with positive thermal expansion, one expects to have

$$\int_V z \rho(z) dz > \int_V z \rho^{(0)}(z) dz. \quad (\text{III.7})$$

This inequality should apply whether the system exhibits a single fluid phase, or coexistence of two fluids with an interface.

#### IV. INTRINSIC DENSITY PROFILE

Presuming that  $N$ ,  $V$ , and  $T$  are such that the system displays liquid-vapor coexistence, the first stage of the process to identify an intrinsic density profile involves locating the relevant Gibbs dividing surface for the macroscopically planar interface. That requires considering the thermodynamic “barometer formula” for the given gravitational field strength  $g$ ,

$$\mu[\rho_g(z|z_G), T] + mgz = C(N). \quad (\text{IV.1})$$

This formula implicitly defines an “ideal” density profile  $\rho_g(z|z_G)$  by use of the uniform-system chemical potential function  $\mu(\rho, T)$  for the substance under consideration. The ideal density profile exhibits a strict density discontinuity (jumping from  $\rho_l$  to  $\rho_v$ ) at some  $z = z_G$ . The constant  $C(N)$  in Eq. (IV.1) is to be chosen so that this ideal density profile represents the proper number of particles between the impenetrable floor (at  $z_f$ ) and ceiling (at  $z_c$ ) of the containing volume:

$$A \int_{z_f}^{z_c} \rho_g(z|z_G) dz = N. \quad (\text{IV.2})$$

Once the Gibbs dividing surface has been located at  $z_G$ , the “ideal” formal numbers of particles  $N_l^*$  and  $N_v^*$  belonging, respectively, to the liquid and vapor phases can be assigned,

$$N_l^* = A \int_{z_f}^{z_G} \rho_g(z|z_G) dz, \quad (\text{IV.3})$$

$$N_v^* = N - N_l^* = A \int_{z_G}^{z_c} \rho_g(z|z_G) dz.$$

It must be stressed these numbers are not the averages that would be inferred from the actual continuous density profile  $\rho(z)$  below and above  $z_G$ , specifically,

$$N_l = A \int_{z_f}^{z_G} \rho(z) dz, \quad (\text{IV.4})$$

$$N_v = N - N_l = A \int_{z_G}^{z_c} \rho(z) dz.$$

Surface roughening (including but not necessarily restricted to “capillary waves”) that locally deforms the interface position has the net effect of removing particles from the dense liquid just below  $z_G$  and placing them in the vapor-phase domain just above that dividing surface. This tendency is illustrated schematically in Fig. 1. Consequently, one has

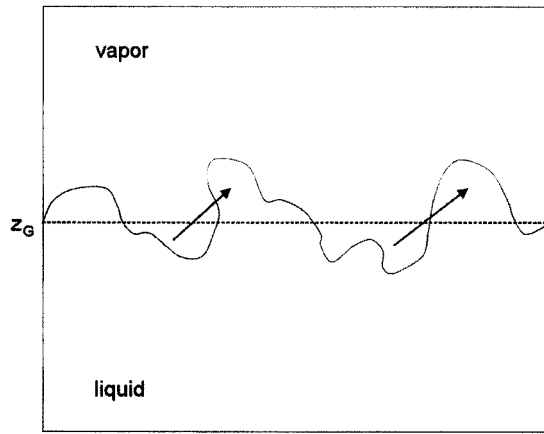


FIG. 1. Schematic view of liquid-vapor surface roughening due to various thermal activation processes. As indicated by the arrows, the particle population in the dense liquid phase below the dividing surface at height  $z_G$  (dashed line) is depleted by the roughening, and the vapor phase population above  $z_G$  is correspondingly increased.

$$N_l = N_l^* - D, \quad (IV.5)$$

$$N_v = N_v^* + D,$$

where  $D > 0$ .

Because the steepest descent mapping to inherent structures modifies the density profile, in order to maintain exactly  $N_l$  particles below and  $N_v$  particles above the formal dividing surface after mapping, it is necessary to displace that dividing surface from position  $z_G$  to a different position, say,  $z_G^{(0)}$ . This new location needs to be uniquely selected to satisfy the analog of Eq. (IV.4),

$$N_l = A \int_{z_f}^{z_G^{(0)}} \rho^{(0)}(z) dz, \quad (IV.6)$$

$$N_v = N - N_l = A \int_{z_G^{(0)}}^{z_c} \rho^{(0)}(z) dz.$$

In view of inequality (III.7), one expects normally to have  $z_G > z_G^{(0)}$ .

Once the displaced dividing surface has been fixed at  $z_G^{(0)}$ , it becomes possible to classify inherent structures according to how they individually partition particles above and below that surface. The numbers  $N_l$  and  $N_v$  represent averages over all inherent structures; any specific example can deviate from those averages. In carrying out that classification, it makes sense to treat together all geometrically equivalent inherent structures that differ only by particle permutations, and index  $\alpha$  will refer to these equivalence sets. The mapped density profile  $\rho^{(0)}(z)$  can be resolved into contributions arising from each  $\alpha$ ,

$$\rho^{(0)}(z) = \sum_{\alpha} P_{\alpha} \rho_{\alpha}^{(0)}(z), \quad (IV.7)$$

where  $P_{\alpha}$  is the occupancy probability (unaffected by the steepest descent mapping) for the basin set identified by  $\alpha$ , and  $\rho_{\alpha}^{(0)}(z)$  is the density profile when the system is confined

just to those permutation-equivalent basins for set  $\alpha$ . Using this resolution it is then possible to write

$$A \int_{z_f}^{z_G^{(0)}} \rho_{\alpha}^{(0)}(z) dz = N_l^* - \Delta_{\alpha}, \quad (IV.8)$$

$$A \int_{z_G^{(0)}}^{z_c} \rho_{\alpha}^{(0)}(z) dz = N_v^* + \Delta_{\alpha},$$

thereby defining the cross-dividing-surface particle transfer numbers  $\Delta_{\alpha}$ . Notice that these last equations purposely revert to inclusion of the ideal phase numbers  $N_l^*$  and  $N_v^*$  so that each deviation  $\Delta_{\alpha}$  measures the total matter transfer across the displaced dividing surface.

Define the inherent structure set  $\mathbf{Q}$  to contain all inherent structure permutation equivalences  $\alpha$  for which  $|\Delta_{\alpha}|$  attains its minimum value. The principal reason for this choice is that it effectively selects the included inherent structures to be those with particle distributions that are substantially devoid of cross-surface structural excitations, thus conforming closely to the planar dividing surface at  $z_G^{(0)}$ . Note that a result of including  $N_l^*$  and  $N_v^*$  in the defining Eqs. (IV.8) is that the average value of  $\Delta_{\alpha}$  will be positive,

$$\langle \Delta_{\alpha} \rangle \equiv \sum_{\alpha} P_{\alpha} \Delta_{\alpha} > 0. \quad (IV.9)$$

The set  $\mathbf{Q}$  defines its own average inherent structure density profile,

$$\rho_{\mathbf{Q}}^{(0)}(z) = \left[ \sum_{\alpha \in \mathbf{Q}} P_{\alpha} \rho_{\alpha}^{(0)}(z) \right] / \left[ \sum_{\alpha \in \mathbf{Q}} P_{\alpha} \right]. \quad (IV.10)$$

Because of the way that set  $\mathbf{Q}$  has been defined, this last expression, in fact, serves as an intrinsic profile for the mapped configurations. Of course, the objective has been to identify the appropriate intrinsic density profile for the premapped ensemble. That follows immediately by thermally re-exciting the members of set  $\mathbf{Q}$  each within their own basins, whereupon each  $\rho_{\alpha}^{(0)}(z)$  transforms to its own  $\rho_{\alpha}(z)$ . These latter functions satisfy the thermally re-excited analog of prior Eq. (IV.7),

$$\rho(z) = \sum_{\alpha} P_{\alpha} \rho_{\alpha}(z). \quad (IV.11)$$

Consequently, this analysis leads to the following expression for the intrinsic density profile:

$$\rho_{\mathbf{Q}}(z) = \left[ \sum_{\alpha \in \mathbf{Q}} P_{\alpha} \rho_{\alpha}(z) \right] / \left[ \sum_{\alpha \in \mathbf{Q}} P_{\alpha} \right]. \quad (IV.12)$$

This point of view carries the implication that capillary wave excitations of the interface necessarily require interbasin transitions out of the basins for the distinguished set  $\mathbf{Q}$ , and should not be attributed simply to intrabasin vibrations. An experimental study of the dynamics of capillary waves on glycerol, and their dramatic slowing upon temperature reduction, supports this proposition.<sup>28</sup> Following the procedure just outlined, careful future simulations of simple liquid models such as that with the Lennard-Jones 12,6 pair potential should be able to determine an intrinsic profile  $\rho_{\mathbf{Q}}(z)$  quantitatively, and to determine the extent to which an

dated van der Waals theory produces an interface profile approximating that  $\rho_{\mathbf{Q}}(z)$  in the  $g \rightarrow 0$  limit.

Considering the fact that requiring  $\alpha \in \mathbf{Q}$  constitutes a constraint on interfacial configurations, and that removing this constraint should lower the interfacial free energy, one has the following inequality applicable below the critical temperature between the respective surface tensions for the unconstrained interface ( $\gamma$ ), and for the intrinsic density profile [ $\gamma^{(0)}$ ],

$$\gamma < \gamma^{(0)}. \quad (\text{IV.13})$$

It might seem natural to identify the intrinsic surface tension  $\gamma^{(0)}$  with the phenomenological parameter  $\gamma_0$  invoked by the capillary wave approach, and appearing in Eq. (II.7), however, this requires an independent verification.

## V. CAPILLARY WAVE IDENTIFICATION PROBLEM

Having defined an intrinsic density profile through identification of the subset  $\mathbf{Q}$  of inherent structures, any analysis directed toward identifying capillary waves naturally would attempt to assign wave amplitudes to inherent structures belonging to sets  $\alpha' \notin \mathbf{Q}$ . This needs to be done while recalling that lateral-direction periodic boundary conditions apply to the system, implying that all inherent structures are two-dimensional manifolds, not isolated single points, in the multidimensional configuration space. That entails uncertainty in the phases of the component waves. However, it should suffice to find an assignment procedure that is applicable to just one of the points of the manifold for any given inherent structure in set  $\alpha'$ . An alternative tactic would be to replace the lateral periodicity with vertical impenetrable walls at the sides of the interface system, thus removing the translational invariance.

Ideally, for any given  $\alpha' \notin \mathbf{Q}$  one would like to identify a “best” approximation to that inherent structure in terms of a lateral-position-dependent vertical displacement of the intrinsic density profile, i.e., an approximation of the form  $\rho_{\mathbf{Q}}^{(0)}[z + \delta z(x, y)]$ , where

$$\delta z(x, y) = \sum_{|\mathbf{k}| \leq k_u} [a(\mathbf{k}) \sin(k_x x + k_y y) + b(\mathbf{k}) \cos(k_x x + k_y y)]. \quad (\text{V.1})$$

Here, the coefficients  $a(\mathbf{k})$  and  $b(\mathbf{k})$  would be treated as adjustable parameters to optimize the fit, and an upper limit  $k_u$  on the Fourier series has been imposed to conform with Eq. (II.8) above. If this optimization were carried out for a substantial collection of inherent structures in various sets  $\alpha' \notin \mathbf{Q}$ , one could then in principle analyze the results statistically to gauge the extent of independence and of Gaussian distribution characteristics for the coefficients as presumed by the capillary wave picture.

Unfortunately, there are several significant basic and practical shortcomings to this strategy. To be consistent with the intrinsic profile definition advanced in Sec. IV above, no arbitrary parameters that are not present in the system Hamiltonian should be allowed to intrude, and this constitutes a powerful constraint. In particular, there appears to be no unique method to determine optimal coefficients in the series

(V.1) that successfully isolates surface-wave fluctuations from bulk-phase fluctuations. For example, considering just a macroscopically thin layer of material around the center of the interface requires assigning a layer width at the outset, thus violating the constraint. Similarly, there exists no precise and objective criterion derivable only from the Hamiltonian for selection of the wavevector upper cutoff  $k_u$ .

However, in spite of these negative observations, a full and literal interpretation of inherent structures according to detailed capillary wave theory is not necessary to justify its principal qualitative implications. These implications really rely principally on the influence of surface waves approaching the long-wavelength limit, where macroscopic behavior becomes relevant. An indirect but obvious indicator of the relevance of long-wavelength capillary waves for interface structure, whether in experiment or numerical simulation, would be to document sensitivity to the gravitational (or centrifugal) field strength  $g$ . This justifies effort to augment conventional terrestrial experiments with those in a space station environment (low  $g$ ) and in centrifuges (high “ $g$ ”). Specifically, one would look for verification of the interface width logarithmic functional dependence on  $g$  conveyed by Eqs. (II.9) and (II.10). That logarithmic behavior should survive steepest descent mapping to inherent structures, and so should be observable in simulations as the  $g$  dependence both of the pre- and postmapped density profiles  $\rho(z, g)$  and  $\rho^{(0)}(z, g)$ . Another indirect indicator would be to search for lateral density-density pair correlations in the interface, to which capillary wave excitations supply characteristic contributions that become longer and longer ranged as  $g \rightarrow 0$ .<sup>12,29</sup> Because these properties arise from long-wavelength surface waves, they do not require that all capillary waves over some nonzero interval  $0 < |\mathbf{k}| < k_u$  act strictly as independent normal surface modes.

## VI. CONCLUDING REMARKS

The principal objective pursued in this paper is the conceptual identification of an intrinsic density profile for the liquid-vapor interface in a many-particle system that is subject to an arbitrary gravitational field strength  $g$  (or its centrifugal equivalent). The basic approach used for this analysis was mapping of an ensemble of thermal equilibrium configurations onto potential energy minima, “inherent structures.” A well-defined subset of these inherent structures, after rethermalization, provides the intrinsic density profile. This procedure is implemented without artificially introducing any parameters (such as energy or length scales) that are not present within the system Hamiltonian itself or the thermodynamics that it generates. Although the present analysis has been presented as an exercise in classical statistical mechanics, it needs to be emphasized that the general inherent structure formalism also extends into the quantum regime,<sup>30</sup> so that the approach presented above can be modified to account for quantum corrections.

By construction, this intrinsic density profile should have a well-defined limit as  $g \rightarrow 0$ , provided that the temperature is below the critical temperature for the substance of interest. To this extent, it apparently agrees qualitatively with the

character of the density profile produced by interface theories of the van der Waals type. However, this eliminates those surface-wave fluctuations that the capillary wave theory predicts will cause the interface width to diverge logarithmically as  $g \rightarrow 0$ . While it may be possible to identify a convolution smoothing operation which accurately converts the localized intrinsic density profile  $\rho_{\mathbf{Q}}(z, g)$  to the broader thermally averaged profile  $\rho(z, g)$ ,

$$\rho(z, g) \equiv \int_{z_f}^{z_c} K(z - z', g) \rho_{\mathbf{Q}}(z', g) dz',$$

$$\int_{-\infty}^{+\infty} K(y, g) dy = 1,$$
(VI.1)

and while this smoothing may indeed produce qualitatively the same logarithmic broadening as the capillary wave approximation, for reasons stressed above it is unclear how this convolution operation can arise from a full set of strictly independent capillary wave amplitudes attributable to any arbitrarily chosen inherent structure. Nevertheless, it should be clear that computer simulation studies incorporating wide ranges in  $g$  could play an important future role in producing intrinsic density profiles for simple model many-particle systems, and for testing the dependence of the nonintrinsic interface width on the magnitude of  $g$ .

The elementary forms of both the van der Waals and the capillary wave interface theories produce monotonic density profiles, Eqs. (II.5) and (II.10). Nevertheless, it is important to realize that experiments have indicated that under some circumstances oscillatory density profiles exist at liquid-vapor interfaces. This was first observed for liquid metals,<sup>31,32</sup> for which the conduction electrons appear to provide the necessary surface layering effect.<sup>33</sup> More recently, a similar oscillatory density profile has been observed for an insulating molecular liquid, "TEHOS."<sup>34</sup> Whatever layering might be present in an equilibrium profile, reduction to the intrinsic profile by the analysis described above should have the effect of amplifying the spatial oscillations. Note that the approach outlined in this paper, even when applied to structureless particles, does not exclude intrinsic density profiles with nonmonotonic layered shapes.

The basic concepts used here to identify an intrinsic profile for single-component systems exhibiting liquid-vapor coexistence can easily be extended to multicomponent systems. These can include both liquid-vapor coexistence, with multiple species coexisting in both fluid phases, as well as immiscible pairs of dense liquids. However, such extensions

require deciding which of the species  $i$  is the one whose inherent excess quantity  $\Delta_{\alpha}^{(i)}$  is to be used to define the inherent structure subset  $\mathbf{Q}$ , in analogy to Eqs. (IV.8) for the single-component case. In general, different choices of that species  $i$  will produce different intrinsic profiles for all of the species present, but for any choice the resulting intrinsic profile widths should remain bounded as  $g \rightarrow 0$ , provided that the system is not at a critical point.

<sup>1</sup>S. Ono and S. Kondo, *Encyclopedia of Physics*, edited S. Flügge (Springer, Berlin, 1960), Vol. 10, p. 134.

<sup>2</sup>R. Evans, *Adv. Phys.* **28**, 143 (1979).

<sup>3</sup>J. S. Rowlinson and B. Widom, *Molecular Theory of Capillarity* (Clarendon, Oxford, 1982).

<sup>4</sup>F. H. Stillinger and T. A. Weber, *Phys. Rev. A* **25**, 978 (1982).

<sup>5</sup>F. H. Stillinger and T. A. Weber, *Phys. Rev. A* **28**, 2408 (1983).

<sup>6</sup>F. H. Stillinger, *Phys. Rev. E* **59**, 48 (1999).

<sup>7</sup>D. J. Wales, *Energy Landscapes* (Cambridge University Press, Cambridge, England, 2003).

<sup>8</sup>J. D. van der Waals, Verh. K. Akad. Wet. Amsterdam, Afd. Natuurkd. **1**, 56 (1893).

<sup>9</sup>L. Mandelstam, *Ann. Phys.* **41**, 609 (1913).

<sup>10</sup>F. P. Buff, R. A. Lovett, and F. H. Stillinger, *Phys. Rev. Lett.* **15**, 621 (1965).

<sup>11</sup>J. S. Rowlinson and B. Widom, *Molecular Theory of Capillarity* (Clarendon, Oxford, 1982), p. 31.

<sup>12</sup>J. D. Weeks, *J. Chem. Phys.* **67**, 3106 (1977).

<sup>13</sup>F. H. Stillinger, *J. Chem. Phys.* **76**, 1087 (1982).

<sup>14</sup>F. H. Stillinger, *Int. J. Quantum Chem., Quantum Chem. Symp.* **16**, 137 (1982).

<sup>15</sup>E. Chacón and P. Tarazona, *Phys. Rev. Lett.* **91**, 166103 (2003).

<sup>16</sup>A. Lastri, F. Dalfovo, L. Pitaevskii, and S. Stringari, *J. Low Temp. Phys.* **98**, 227 (1995).

<sup>17</sup>J. S. Rowlinson and B. Widom, *Molecular Theory of Capillarity* (Clarendon, Oxford, 1982), Chap. 3.

<sup>18</sup>J. S. Huang and W. W. Webb, *J. Chem. Phys.* **50**, 3677 (1969).

<sup>19</sup>E. S. Wu and W. W. Webb, *Phys. Rev. A* **8**, 2065 (1973).

<sup>20</sup>S. Fisk and B. Widom, *J. Chem. Phys.* **50**, 3219 (1969).

<sup>21</sup>T. Svedberg and K. O. Pedersen, *The Ultracentrifuge* (Clarendon, Oxford, 1940).

<sup>22</sup>G. Baym and F. K. Lamb, in *Encyclopedia of Physics*, 3rd ed., edited by R. G. Lerner and G. L. Trigg (Wiley-VCH, Weinheim, 2005), Vol. 2, p. 1722.

<sup>23</sup>J. V. Sengers, J. M. J. Van Leeuwen, and J. W. Schmidt, *Physica A* **172**, 20 (1991).

<sup>24</sup>J. W. Schmidt, *Physica A* **172**, 40 (1991).

<sup>25</sup>F. H. Stillinger and T. A. Weber, *Phys. Rev. A* **25**, 978 (1982).

<sup>26</sup>F. H. Stillinger and T. A. Weber, *Phys. Rev. A* **28**, 2408 (1983).

<sup>27</sup>P. G. Debenedetti and F. H. Stillinger, *Nature (London)* **410**, 259 (2001).

<sup>28</sup>T. Seydel, A. Madsen, M. Tolan, G. Grübel, and W. Press, *Phys. Rev. B* **63**, 073409 (2001).

<sup>29</sup>D. Bedeaux and J. D. Weeks, *J. Chem. Phys.* **82**, 972 (1985).

<sup>30</sup>F. H. Stillinger, *J. Chem. Phys.* **89**, 4180 (1988).

<sup>31</sup>O. M. Magnussen *et al.*, *Phys. Rev. Lett.* **74**, 4444 (1995).

<sup>32</sup>M. J. Regan *et al.*, *Phys. Rev. Lett.* **75**, 2498 (1995).

<sup>33</sup>S. A. Rice *et al.*, in *Advances in Chemical Physics*, edited by I. R. Prigogine and S. A. Rice (Wiley, New York, 1974), Vol. XXVII.

<sup>34</sup>H. Mo *et al.*, *Phys. Rev. Lett.* **96**, 096107 (2006).